1. Cover Page

Federal Agency:	Department of Energy – National Energy Technology Lab
Federal Grant Number:	DE-FE0026192
Project Title:	Enhancing High Temperature Anode Performance with 2° Anchoring Phases
PI Name:	Dr. Robert Walker, Professor rawalker@montana.edu (406) 994-7928
Team Members:	Dr. Stephen Sofie, Associated Professor ssofie@montana.edu (406) 994-6299 Dr. Roberta Amendola, Assistant Professor Roberta.amendola@montana.edu (406) 994-6296

Name of Submitting Official: Traci Miyakawa

DUNS Number: 625447982

Recipient Organization: Montana State University

Project Period: 10/1/2015 – 3/31/2017 (NCE through 7/31/2017)

Reporting Period End Date: 7/31/2017

Report Term: Final

Disclaimer:

Signature of Submitting Official: 

2. Accomplishments.

2a. What are the major goals of the project?

This project's objectives are to test and refine the hypothesis that judiciously chosen, minority 2˚ phases can enhance SOFC anode performance and durability by preventing sintering of small particle catalysts and by strengthening the mechanical properties of the anode iteslf. Preliminary data demonstrated that this hypothesis is plausible, although the mechanism(s) responsible for improvements in flexural strength and resistance to degradation remain unresolved. Specific objectives include the following:

- Identifying the most effective means of introducing 2˚ phase precursors to traditional Ni-YSZ cermet structures (mechanical mixing or solution phase infiltration) and the optimal 2˚ phase loadings
- Determining the optimal thermal conditioning procedures that promote 2˚ phase formation while introducing as little perturbation as possible to anode microstructure.
- Quantifying explicitly the effects of 2˚ phases on the electrochemical performance and durability of SOFC anodes using a suite of *in operando* and *ex situ* techniques.

Meeting these objectives will afford a complete, materials specific picture of how 2˚ phase formation affects SOFC anode properties The research program described in this section is focused primarily on applied laboratory or bench-scale research and development. The criteria that will determine whether or not our strategies are successful are simple to articulate:

- Are anodes containing 2˚ phases stronger than anodes without the 2˚ phases?
- Do anodes containing 2˚ phases outperform and last longer than anodes without 2˚ phases?

Answering these questions requires simple measurements: fracture testing and persistent electrochemical monitoring *in operando*. Specific project objectives fall into three general categories: 1) fabricating anodes; 2) testing membrane electrode assembly mechanical strength; and 3) performing *in operando* electrochemical and spectroscopic studies. During the first quarter of this project, considerable headway has been made in categories (1) and (2) as detailed below. Beginning experiments to meat the goals of category (3) will require successful development of a membrane electrode preparation procedure.

2b. What was accomplished under these goals?

This project accomplished all of its goals at the end of the award period. Specifically, accomplishments included developing and optimizing strength testing of aluminum titanate (ALT)-doped Ni-YSZ materials and identified the dopant levels that optimized mechanical strength and enhanced electrochemical performance. We also optimized our ability to fabricate electrolyte supported button cells with anodes consisting of powders provided by Fuel Cell Energy. In several instances, those anodes were infiltrated with ALT and tested with hydrogen for 30 hours at 800˚C at an applied potential of 0.4 V.

Our research activities were focused in three areas: 1) mechanical strength testing on as prepared and reducced nickel-YSZ structures that were either free of a dopant or prepared by mechanically mixing in ALT at various weight percents (up to 10 wt%); 2) 24-hour electrochemical testing of electroylte supported cells having anodes made from Ni/YSZ and Ni/YSZ/ALT anodes with

specific attention focused on modeling degradation rates; and 3) *operando* EIS and optical testing of both in-house fabricated devices as well as membrane electrode assemblies that were acquired from commercial vendors. Relevant activities are described in detail below. The sections below highlight and summarize accomplishments achieved during this project. Specific details about any given activity can be found in the relevant project quarterly reports.

Task 2.2.1 Fracture Strength Evaluation and 2.2.3 Fractography

Mechanical properties analysis of brittle materials is crucial for Solid Oxide Fuel Cell (SOFC) development as these properties will determine the lifetime of the ceramic components. Manufacturing mechanically strong materials will lead to longer lifetimes of the SOFCs. Necessity for longevity of these cells has led to work in development of mechanically strong ceramic and cermet materials for SOFC components.

This work studied the mechanical properties of Aluminum Titanate, Al_2TiO_5, (ALT) dopant on common anode material, NiO and YSZ. This summary will begin with discussion of sample manufacturing and testing. Discussion of mechanical properties of the doped anodes tested will be discussed with emphasis on comparisons of different batches.

Sample Bars Manufacturing and Fractography

To evaluate the fracture strength of the anode materials, the manufacturing of rectangular bars was necessary. Sample bars size of 30x5x2 mm was selected following the ASTM standard C1161-13 -Test Method for Flexural Strength of Advanced Ceramics at Ambient Temperature. The pressing die had (Figure 1 a and b) tolerances of 0.05 mm.

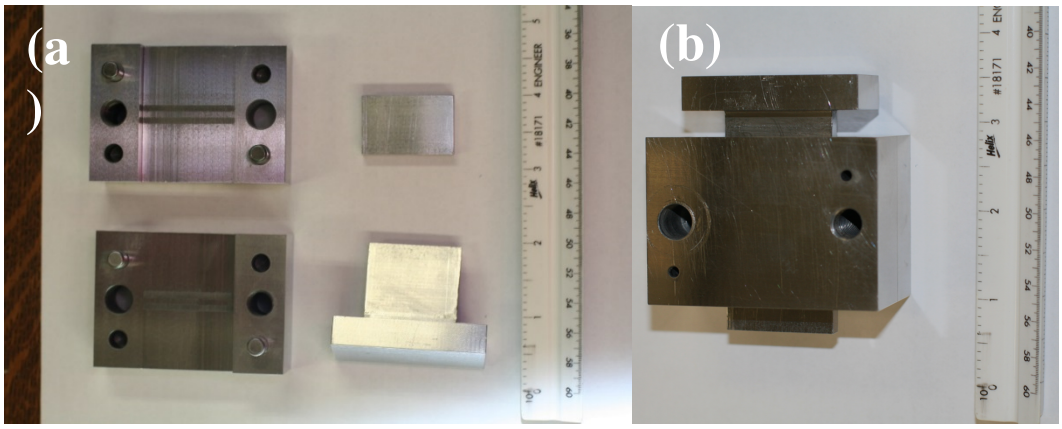

Figure 1: Open die (a) and assembled die (b)

Several parameters of the pressing process were investigated in order to establish a standard pressing protocol and the manufacturing of defect free bars:

1. Influence of the pressing load
2. Influence of the pressing time
3. Influence of binder addition

NiO-YSZ was selected as prototyping material to optimize the pressing protocol. The ratio between the NiO and the YSZ powders was 66 wt% to 34 wt%, respectively. The powders were ball milled for at least 24 hours, flash frozen in liquid nitrogen and freeze dried.

After pressing the green samples were sintered at 1400°C for 5 hours with a heating/cooling ramp of 5°C/min.
FE-SEM image analyses were performed on sintered samples surfaces and cross sections to evaluate the microstructure and defect distribution. Figure 2 is an example of a pressed and sintered sample.

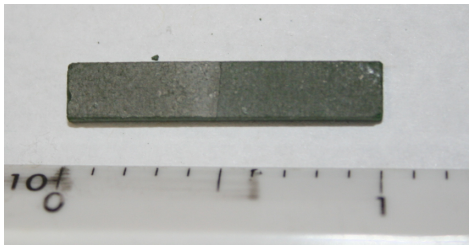

Figure 2: example of pressed and sintered sample

Investigation into the pressing process found that optimal pressing load was 5,000 lbf (22,240 N) with a pressing time of 1 minute. Binder addition was determined to be optimal for 5 wt% addition of polyethylene glycol (PEG). Binder was added during the ball milling stage to allow for homogeneous mixture of the material. With the addition of binder, a burn out run was added before the sintering cycle which consisted of a ramp to 450°C at a rate of 2 °C/min with a dwell of 2 hours. After this, sintering was conducted following the above-mentioned cycle.

Fracture Strength Evaluation
Brittle materials are commonly tested in bending under combined tensile/compressive stresses. The rectangular samples were tested in a three-point flexural fixture (bending test) in order to evaluate the resulting Modulus of Rupture (MOR). A higher MOR corresponds to a mechanically stronger material. Figure 3 shows a picture and schematic of the testing apparatus.

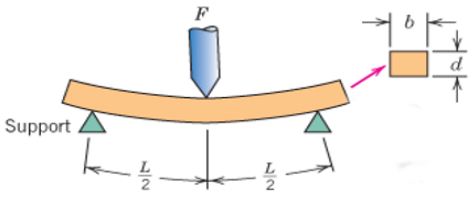

$$\sigma_{fs} = \frac{3F_f L}{2bd^2}$$

F_f = applied load at failure

σ_{fs} = flexural strength or Modulus of rupture

Figure 3: Picture and schematic of the three-point bending apparatus

Batches of 30 samples each were sintered to be mechanically tested. Width and thickness were recorded prior to fracture. The force (N) and displacement at fracture were also recorded and used to calculate the material Weibull exponent. The equation for the calculation of the Modulus of Rupture can be found below as Equation 1.

$$MOR = \frac{3FL}{2bT^2} \qquad Equation\ (1)$$

F is the force at fracture (N), L is the length between the two supporting posts (m), b is the sample width (m), and T is the sample thickness (m). After assessing the MOR, the Weibull exponent "m" was evaluated using the equation below.

$$p(s) = e^{-(\frac{\sigma}{\sigma_0})^m} \qquad Equation\ (2)$$

"m" indicates the nature, severity and dispersion of flaws. A low "m" value indicates non-uniform distribution of highly variable crack length corresponding to broad MOR distribution, while a high "m" value implicates uniform distribution of highly homogeneous flaws with narrow MOR distribution. Typically, for structural ceramics, "m" varies between 3 and 12, depending on the processing conditions. From equation 2, σ is the MOR and σ_0 is a reference strength considering MOR evaluated with 1/e.

Fractography and Mechanical Properties

After sintering, samples were fractured using the above described three-point bending test. Each batch of 30 samples was analyzed using Weibull statistics and fractography was performed on the samples with the highest and lowest strength.

Comparison Analysis of Nano NiO-YSZ (Oxidized)

Figure 4 a-f shows the nano NiO-YSZ with 0, 1, 2.5, 5, 7, and 10 wt% ALT. The increasing amount of the new rough phase (red circle) can be correlated with higher amounts of ALT. Table 1 summarizes the mechanical properties. There is an increasing trend in the average MOR from 0 to 10 wt% ALT. The standard deviation is relatively consistent with the exception of the 10 wt% batch. Also, the Weibull modulus seems to improve until the 10 wt% samples.

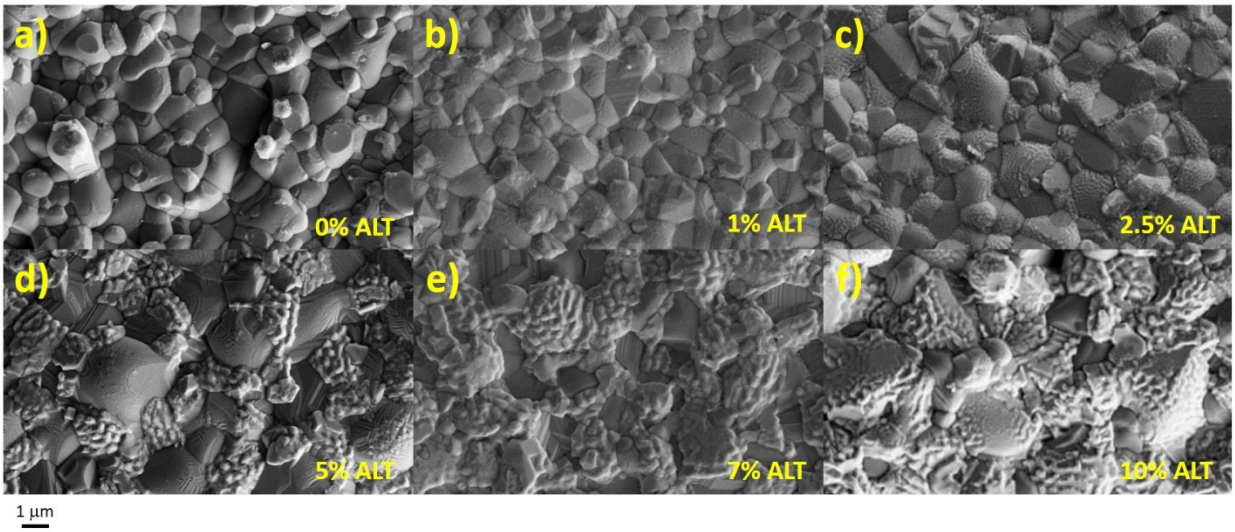

Figure 4a-f: FEM of surface of nano NiO-YSZ + 0, 1, 2.5, 5, 7 and 10 wt% ALT

Table 1: Mechanical Properties of nano NiO-YSZ

	0% ALT	1% ALT	2.5% ALT	5% ALT	7% ALT	10% ALT
Average MOR	121 MPa	164 MPa	169 MPa	191 MPa	197 MPa	236 MPa
Standard Deviation	26.6	28.6	30.8	29.7	31.5	47.2
Weibull Modulus	5.59	6.92	6.55	7.48	7.32	5.89

Comparison Analysis of Micro NiO-YSZ (Oxidized)

For the micro NiO-YSZ, there is a slightly different outcome. Figure 5 a-f below shows the surface images of the micro NiO-YSZ samples with 0, 1, 2.5, 5, 7 and 10 wt% ALT. With increasing ALT, there is a larger amount of the rough phase present on the surface of the samples. Table 2 below compares all the mechanical properties of the different percentages tested. Unlike the nano NiO powder, there seems to be a specific amount of ALT for best mechanical properties corresponding to 5% ALT. Standard deviation and the Weibull modulus are the best for the 7 wt% ALT.

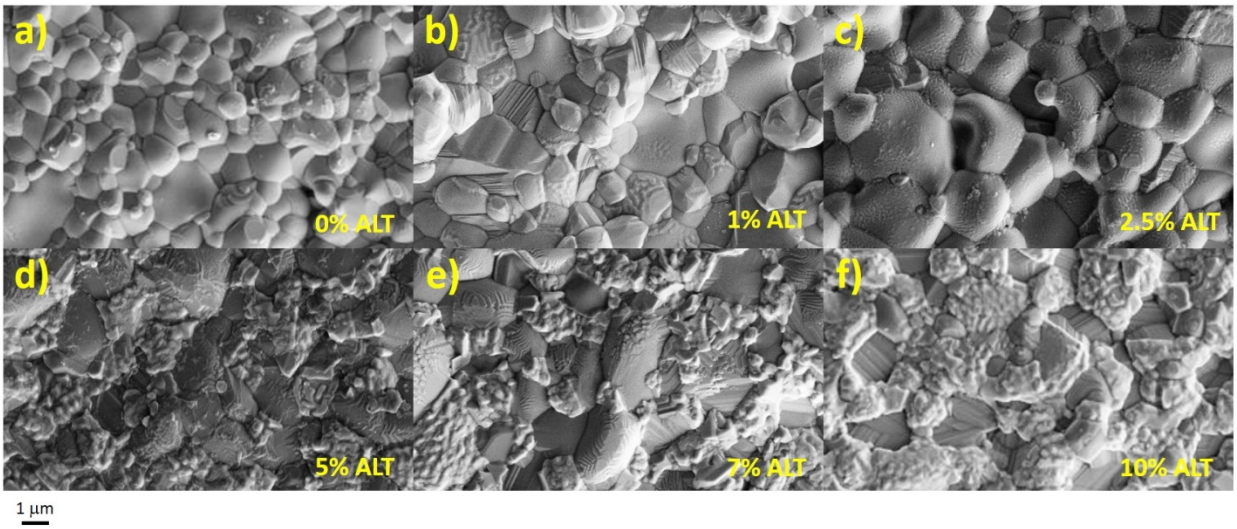

Figure 5a-f: FEM of surface of nano NiO-YSZ + 0, 1, 2.5, 5, 7 and 10 wt% ALT

Table 2: Mechanical Properties of micro NiO-YSZ

	0% ALT	1% ALT	2.5% ALT	5% ALT	7% ALT	10% ALT
Average MOR	100 MPa	136 MPa	185 MPa	226 MPa	191 MPa	150 MPa
Standard Deviation	24.9	44	29.3	29.9	21.4	23.4
Weibull Modulus	5.63	6.92	7.48	6.89	10.61	7.73

Reduction of Anode Material

After completing analysis of the samples that were in their oxidized state, research was conducted on the strength of the samples after reduction in a 5% H_2, 95% N_2 gaseous environment. All samples used for fracture analysis were produced and sintered as per the established process. After sintering, the samples were placed in a tube furnace and reduced at 800°C for 10+ hours. All samples used for the batch were reduced above 97% meaning that 97% of the NiO had converted to Ni metal. The percentage reduction is calculated using the initial and final weight of each sample. After recording the initial weight, the weight is sectioned into its respective components. Once the weight of the NiO is determined in the initial sample, the weight of oxygen can be subtracted using the weight percent of oxygen versus Ni in the NiO crystal. After subtraction of the weight of oxygen, the fully reduced weight can be determined.

Comparison Analysis of Nano Ni-YSZ (Reduced)

Figure 6a-d shows the surface topography of the samples of nano Ni-YSZ ranging from 0 to 10 wt% ALT. The rough phase begins to form after the addition of 1 wt% ALT. The amount of the rough phase (circled in Figure 6c) seems to increase proportionally to the amount of ALT. The small particle cluster phase (circled in Figure 6d) begins to appear after the addition of 5 wt% ALT. The clusters appear to be larger and in higher quantities after the addition of 10 wt% ALT.

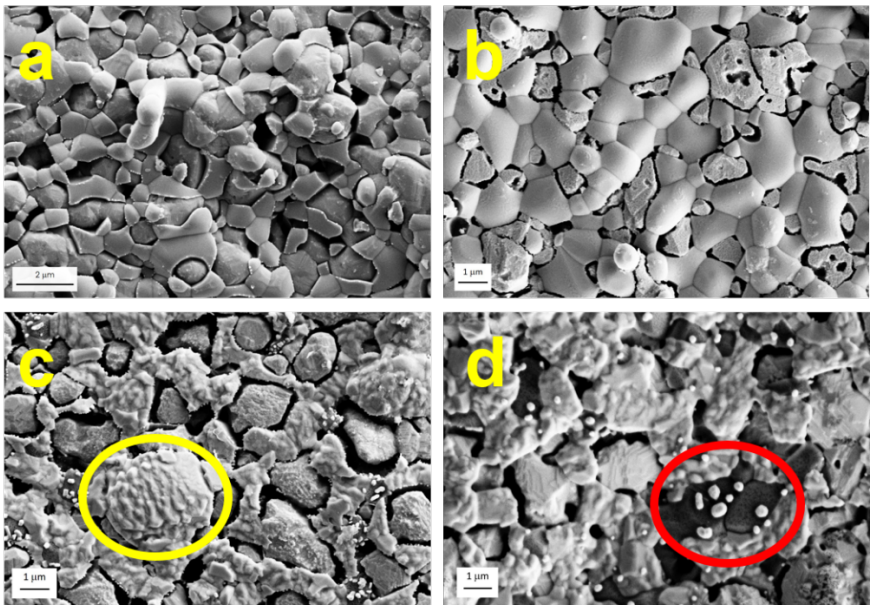

Figure 6a-d: FEM of surface of nano Ni-YSZ + 0, 1, 5, and 10 wt% ALT

Table 3 below shows the mechanical properties data for the nano Ni-YSZ batches. Average MOR is highest for the batch with the addition of 10 wt% ALT. The lowest standard deviation and the highest Weibull modulus was calculated for the batch with the addition of 1 wt% ALT.

Table 3: Nano Ni-YSZ Mechanical Properties

	0% ALT	1% ALT	5% ALT	10% ALT
Average MOR	138 MPa	152 MPa	165 MPa	203 MPa
Standard Deviation	24.3	19.2	22.6	29.1
Weibull Modulus	6.77	9.44	7.48	8.51

Comparison Analysis of Micro Ni-YSZ (Reduced)

Figure 7a-d shows the surface topography of the micro Ni-YSZ samples with varying amounts of ALT. The rough phase (yellow circle) is present after the addition of 1 wt% ALT. Increasing percentages of ALT seems to correlate with an increased amount of the rough phase. The small particle cluster phase is present with the addition of 5 wt% ALT. The phase (red circle) is more distinct with the addition of 10 wt% ALT. Phase characterization will be discussed further below.

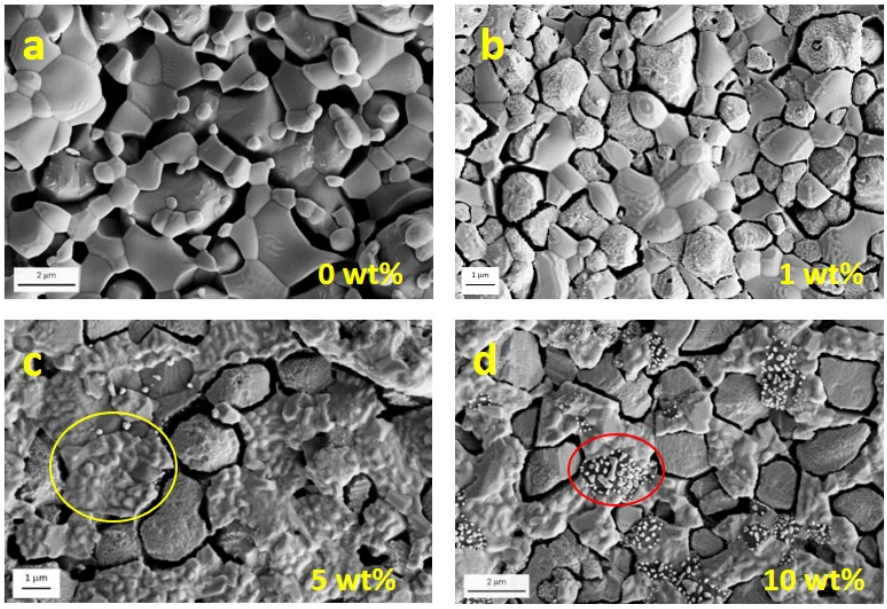

Figure 7a-d: FEM of surface of micro Ni-YSZ + 0, 1, 5, and 10 wt% ALT

Table 4 shows the mechanical properties of the micro Ni-YSZ samples with the various percentages of ALT. The highest average MOR was 187 MPa for the batch with the addition of 10 wt% ALT. The lowest standard deviation and the highest Weibull modulus was calculated also for the batch with 10 wt% ALT. It can be concluded that the addition of 10 wt% ALT produces samples with the most improved mechanical properties.

Table 4: Micro Ni-YSZ Mechanical Properties

	0% ALT	1% ALT	5% ALT	10% ALT
Average MOR	125 MPa	151 MPa	164 MPa	187 MPa
Standard Deviation	21.3	29.1	22.3	17.6
Weibull Modulus	7.49	5.63	8.61	10.61

Auger Nanoprobe Analysis of Micro Ni-YSZ + 10 wt% ALT

In order to determine the nature of the phases present on the surface of the samples with the addition of ALT, the Scanning Auger Nanoprobe (PHI 710) available in the Image and Chemical Analysis Laboratory on the Montana State University campus was used for surface characterization. Auger Electron Spectroscopy (AES) was employed to conduct near surface mapping of a sample of micro Ni-YSZ + 10 wt% ALT. Figure 8a-c shows one map collected with two different element overlays. Figure 8a shows a secondary electron image of the mapped area for comparison of the phases. Figure 8b shows the map with Nickel as blue, Titanium as red, and Aluminum as green. Figure 8c is the same map but Zirconium is blue, Titanium is red, and Aluminum is green. It can be observed that the rough phase seems to consist of zirconium and titanium (circled in Figure 8a). Figure 8b shows that the small particle phase consists of nickel based particles on top of aluminum (circled in Figure 8a).

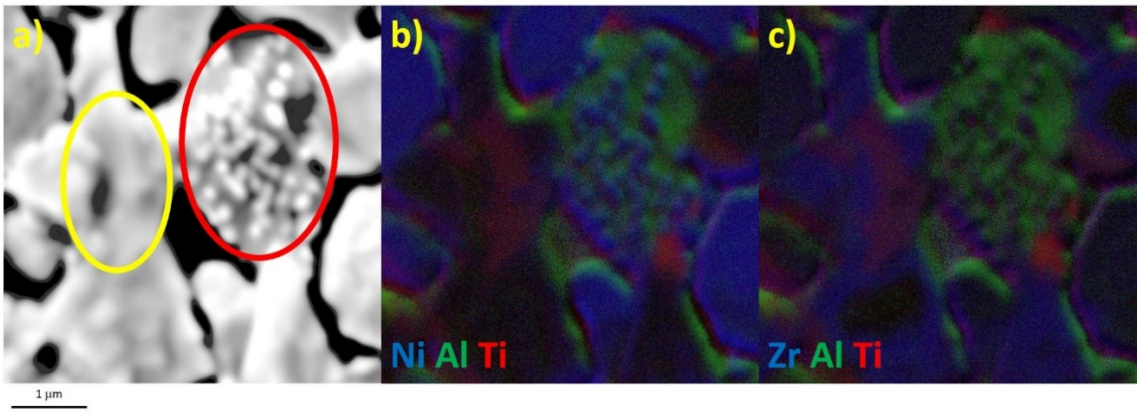

Figure 8 a and b: Auger map of micro Ni-YSZ + 10 wt% ALT

Further analysis of the Auger maps and FEM imaging led to conclusions about the second phase formation and their role in mechanical strengthening. During sintering it is known that ALT decomposes to Al_2O_3 and TiO_2. The rough phase is believed to be the destabilization of YSZ by the addition of TiO_2. Destabilization of YSZ builds a framework for which stress can be distributed in the system aiding in mechanical strengthening. Al_2O_3 reacts with NiO to form $NiAl_2O_4$ during sintering and the addition of $NiAl_2O_4$ is known to cause strengthening of NiO-YSZ system to a point; corresponding to the strength being the highest for the micro oxidized (NiO-YSZ) anodes at 5 wt% ALT. During reduction, some of the $NiAl_2O_4$ reduces allowing for access to Ni-metal that was previously contained in the $NiAl_2O_4$ and this is what the small particle phase is composed of. The addition of Ni-metal adds ductility to the system increasing the mechanical strength; leading to the highest strength seen for the micro reduced (Ni-YSZ), 10 wt% ALT doped samples.

Conclusions

This work concluded that the addition of ALT into the anode material of NiO-YSZ improved the mechanical strength for every addition of ALT. This increased strength could be due to second phase formation as seen with Auger analysis. Increased anode strength allows for thinner anodes in the future with higher strength. With stronger anode material, the longevity of the SOFC cell is increased due to the lower likelihood for cracks to form in the material. The effects of ALT on second phase formation could lead to further material properties tailoring through different doping combinations and concentrations. This research leads to the opportunity for further mechanical properties analysis of ALT doped anode materials in different situations, including redox cycling and thin anodes. Work outlined in this summary has been used for a journal article: M. McCleary, R. Amendola, "Effect of Aluminum Titanate (Al_2TiO_5) Doping on the Mechanical Performance of Solid Oxide Fuel Cell Ni-YSZ Anode", Fuel Cells: from fundamentals to systems, Accepted September 5, 2017.

2.2.2.A Phase I Electrochemical Testing Summary

The effect of the addition of Al_2TiO_5 (ALT) to the anodes of SOFCs made with ~3·µm and ~4·µm initial particle size NiO precursor powder on fuel cell performance has been examined. The determination of optimum ALT amounts to SOFC anodes has been achieved for for SOFC

anodes made with ~4·µm initial particle size NiO precursor powder. Further, it is observed that the addition of ALT to SOFC anodes via infiltration is better at stabilizing performance than the addition of ALT to SOFC anodes via the addition of ALT powder to spray recipes and mechanically mixing in that powder. Finally, it is observed that the performance of fuel cells made with ~3·µm (J.T. Baker green NiO) initial anode NiO powder particle size precursor powder is much more stable than the performance of ~4·µm (Alpha Aesar green NiO) initial anode NiO powder particle size precursor powder.

Figure 9 (left) shows the degradation rates of fuel cells with anodes made from ~4·µm (Alpha Aesar green NiO) initial anode NiO powder particle size precursor powder as a function of the weight percent of the anode ALT addition at 5, 10, 15, and 20 hours. The parabolic dependence of degradation rate on ALT concentration is observed in this figure. The data set at each time was fit with a 2nd order polynomial. The weight percentage of ALT corresponding to the maximum of that data set's parabola was then recorded. The 90% confidence interval of the average of the ALT concentration corresponding to each parabola's maximum was found to be 5.7±0.7 Wt.%, and is shown, along with the fits, in the inset of Figure 9 (left). Figure 9 (right) shows the ALT concentration-degradation relationship that exists for cells with ALT added via mechanical mixing. This figure demonstrates that although the addition of ALT via mechanical mixing improves cell performance, said quantity is not improved in the cells with ALT added via mechanical mixing to the extent that cell performance is improved with ALT addition via infiltration.

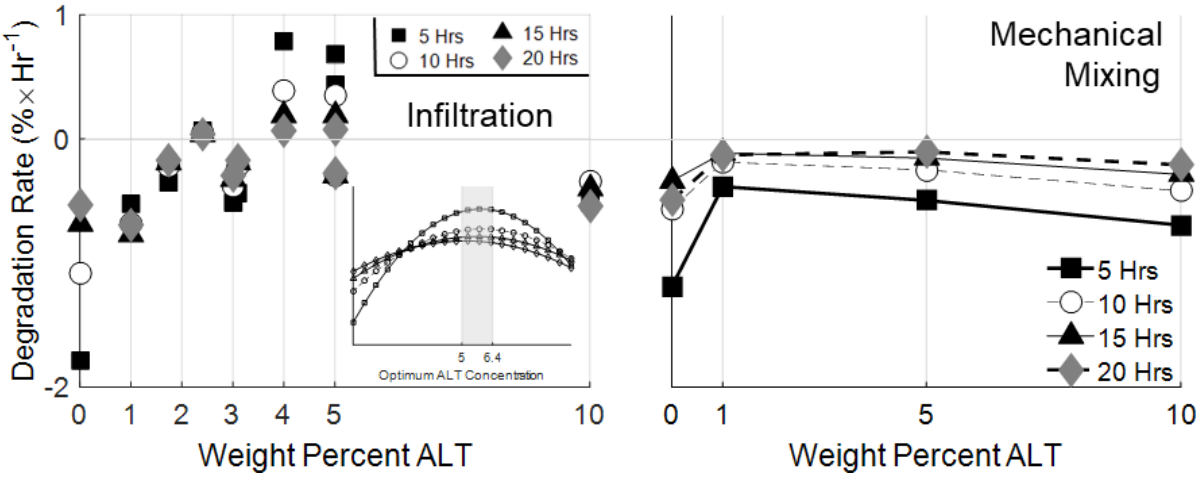

Figure 9: Left: Degradation rates of cells with ALT-infiltrated, ~4·µm initial-particle-size NiO anodes taken at 5, 10, 15, and 20 hours with (inset) plots of second-order polynomial fits of each data set with optimum ALT amount indicated as 5.7±0.7 Wt.% ALT. Right: Degradation rates of cells with ALT addition via mechanical mixing

The estimation of optimim ALT addition was made possible with the employment of a curve-fitting algorithm developed in Matlab during the course of this project. The fuel cell current I as a function of time t was fit to Equation 1 using an in-house produced MatLab algorithm.

$$I(t) = a_0c_0 \cdot \frac{1}{t+1} + a_1c_1 \cdot \sqrt{\frac{t}{t_0-t}} + a_2c_2 \cdot \tan(at-b)^{-1} + a_3c_3 \cdot \frac{I_{Max}}{1+\exp(-at+b)} \quad (1)$$

The user-defined constants a_0, a_1, a_2, and a_3 were chosen as either 1 or 0, and served as "on" or "off" switches for each term in Equation 1. The value of a_3 was set to be opposite of a_2. That is, if a_2 was set to 1, then a_3 was set to zero, and vice versa. The constant t_0 is increased by a set interval each time the appropriate loop of the algorithm was run. The algorithm then determined a value of the coefficient of determination (R^2) for each value of t_0. If the R^2 value of a particular fit was found to be better than the current, best R^2 value, then the associated value of t_0 was kept as the best value of t_0. If the R^2 value associated with any value of t_0 was found to be less than the best R^2 value, then the value of t_0 was assigned to be the value of t_0 associated with the best recorded R^2 value. The best combination of terms for fitting Equation 1 to a particular data set was determined via trial and error. Particularly, the selection of the inverse-tangent function or the logistic equation required more than one attempt at fitting each data set.

The constants a and b were determined using an iterative scheme developed in MatLab. This scheme first determined an optimum value of b using a fixed value of a and five different values of b. The least squares method of curve-fitting was then used to determine values of the constants c_0, c_1, and c_2 or c_3 for each value of b. The corresponding R^2 values for each value of b were found. The relationship defined by the (b, R^2) points was used to define the equation of a parabola given by $R^2 = A_2 \cdot b^2 + A_1 \cdot b + A_0$. Once determined, the coefficients of this parabola were used to define an optimum value of b in Equation 1, given by $b = -A_1/(2 \cdot A_2)$. This optimum value of b was then used as the reference point for defining the next set of five b values. This process was iterated until the change in the R^2 value became less than a user-specified value. This process was then used to determine an optimum value of a. Because changing the value of a changed the optimum value of b, the whole process was iterated several times.

The degradation rate, $R(t) = \frac{dI(t)}{dt}$, of the current is given as Equation 2.

$$R(t) = \frac{-a_0 c_0}{t^2} + \frac{a_1 c_1 \cdot t_0 \sqrt{t_0 - t}}{2\sqrt{t} \cdot (t - t_0)^2} + \frac{a_2 c_2 \cdot a}{(b - at)^2 + 1} + \frac{a_3 c_3 \cdot a \cdot I_{Max} \cdot \exp(b - at)}{(1 + \exp(b - at))^2} \quad (2)$$

The degradation rate of each cell was then normalized with respect to the measured current, $I_{meas}(t)$. This normalized degradation rate, $R_N(t)$, is described mathematically as Equation 3.

$$R_N(t) = \frac{R(t)}{I_{meas}(t)} \quad (3)$$

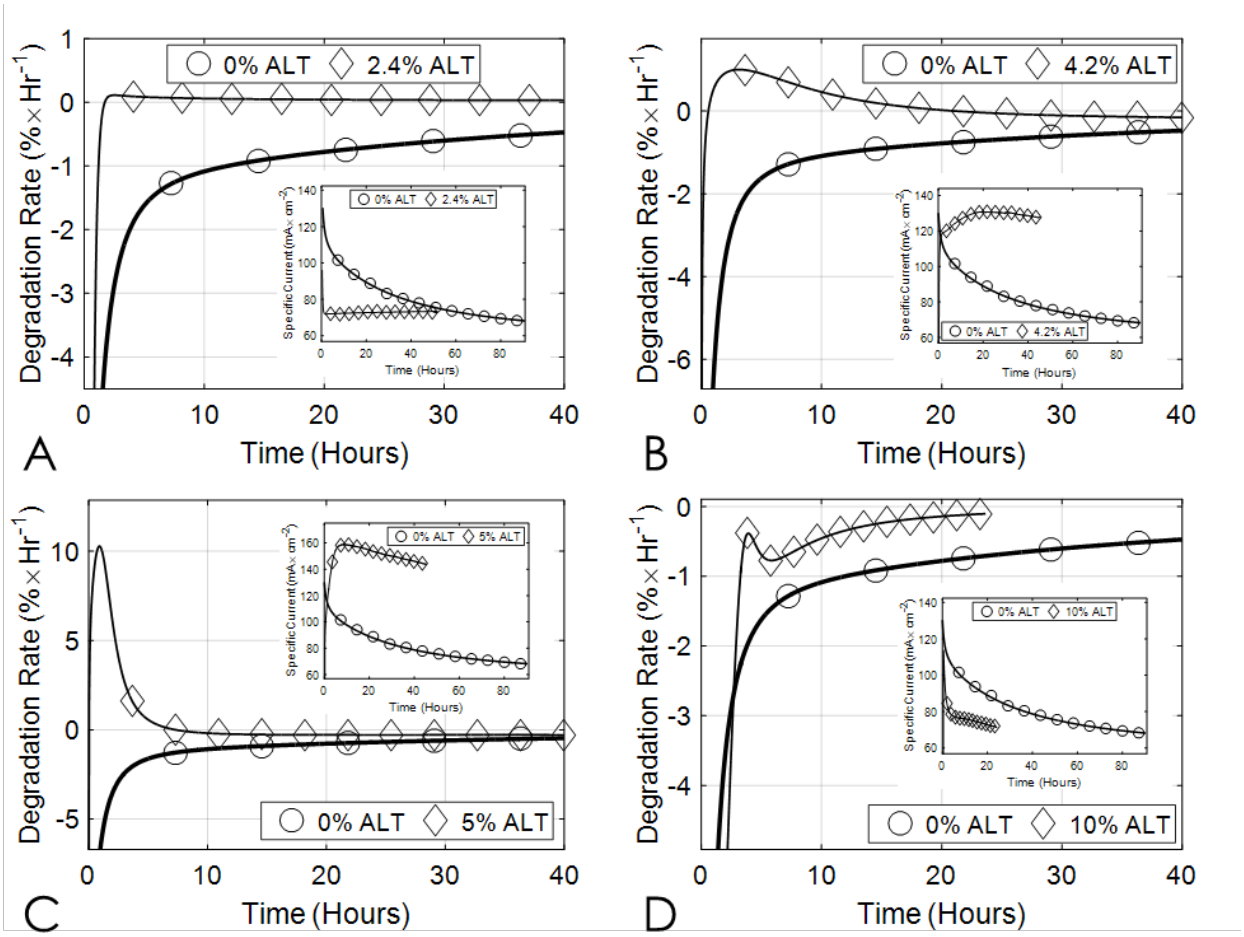

Figure 10: Degradation rates and cell outputs (insets) of (A) 2.4 wt.% ALT, (B) 4.2 wt.% ALT, (C) 5 Wt.% ALT, and (D) 10 wt.% ALT-doped green NiO cells compared with 0 wt.% ALT cell.

Table 5 is included to show a summary of the data presented graphically in Figure 10, as well as a summary of the quality of the curve-fits achieved with the aforementioned algorithm.

Table 5: Degradation rates at 5, 10, 15, and 20 hours

			Degradation Rate (%*Hr^{-1})			
ALT Content (Wt.%)	R-Squared	Max Current (mA/cm^2)	5 Hours	10 Hours	15 Hours	20 Hours
0	0.998	129.318	-1.620	-1.087	-0.901	-0.775
2.4	0.926	93.858	0.082	0.058	0.047	0.041
4.2	0.996	130.847	0.905	0.461	0.175	0.023
5	0.998	159.076	0.565	-0.190	-0.276	-0.292
10	0.988	113.763	-0.695	-0.457	-0.237	-0.143

Figure 11 shows a comparison of cell performance of doped and non-doped fuel cells with anodes made from the ~4·µm (Alpha Aesar green NiO) initial anode NiO powder particle size precursor powder. Parts A, B, C, and D of Figure 2 each show normalized cell degradation rates to 40 hours with measured cell current output shown in the insets. Note that positive and

negative degradation rates imply cell performance increasing and decreasing with time, respectively. Positive and negative values indicate performance gains and losses, respectively. These data suggest that the presence of up to 4% ALT is associated with performance gains in the cell for at least the first five hours. The degradation rates and output currents of select cell performance, shown as insets, are shown as Figure 10.

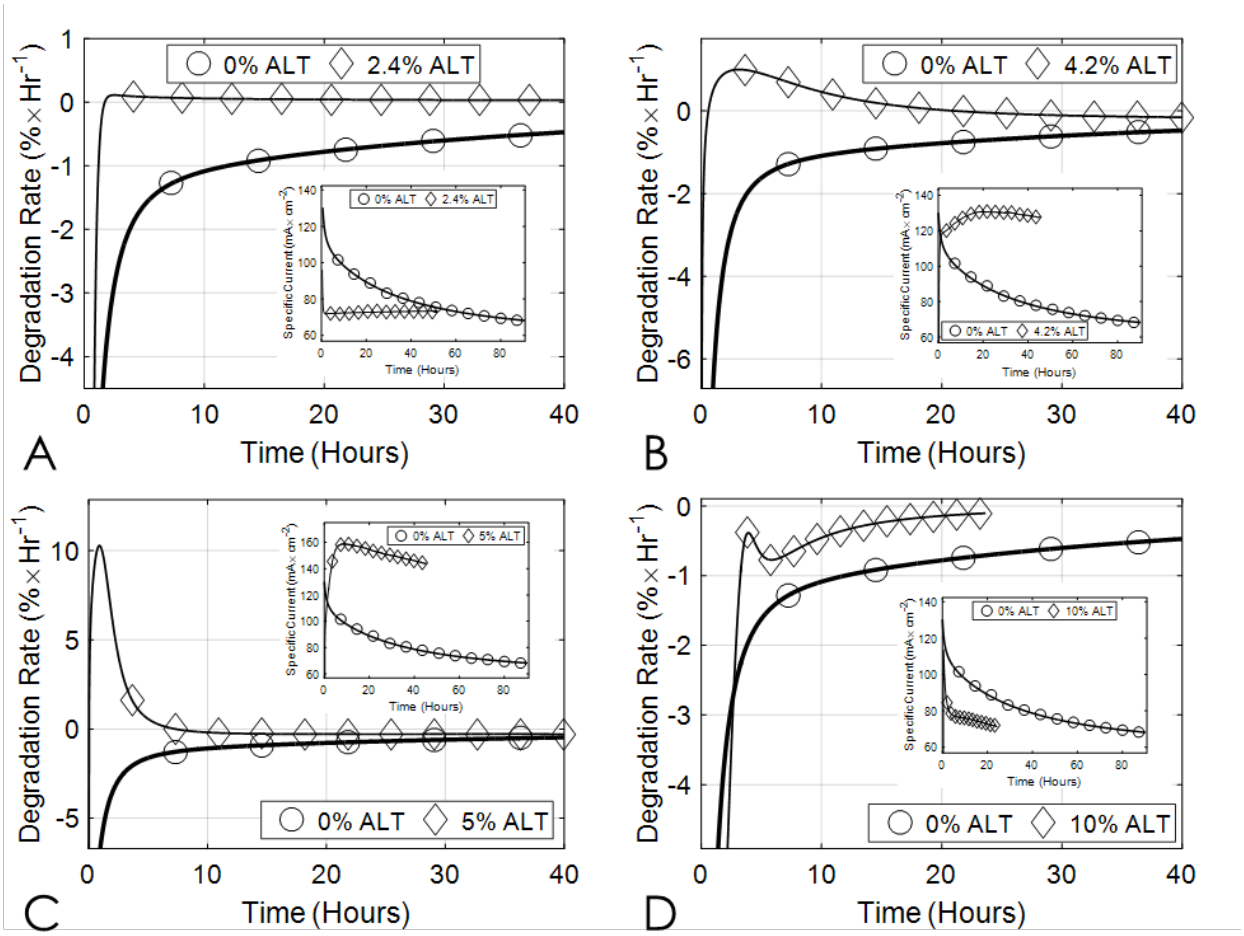

Figure 11: Degradation rates and cell outputs (insets) of (A) 2.4 wt.% ALT, (B) 4.2 wt.% ALT, (C) 5 Wt.% ALT, and (D) 10 wt.% ALT-doped green NiO cells compared with 0 wt.% ALT cell.

Figure 12 (left) shows degradation rates of cells with anodes made from the ~3·µm (J.T. Baker green NiO) initial anode NiO powder particle size precursor powder for cells run longer than 50 hours, but less than 100 hours. Figure 3 (right) shows the same data as Figure 3 (left) for cells run longer than 100 hours. These results suggest the optimal amount of ALT addition to be about 4 Wt.%. This plot also indicates that cells doped with ALT had positive degradation rates beyond 50 hours.

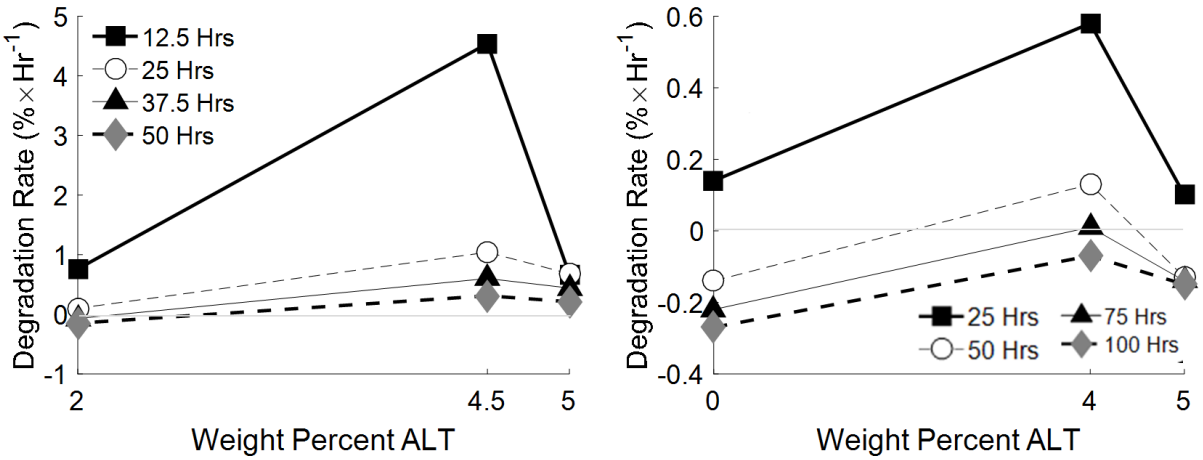

Figure 12: Variation of degradation rates of cells with anodes made from NiO precursors with ~3·µm initial particle size and varying amounts of ALT at (left) 12.5, 25, 37.5, and 50 hours and (right) 25, 50, 75, and 100 hours

Figures 13(A) and 13(C) show measured current outputs of cells made with ~3·µm (J.T. Baker green NiO) initial anode NiO powder particle size precursor powder. Figures 13(B) and 13(D) show the corresponding degradation rates of the current outputs shown in Figures 13(A) and 13(C), respectively. The inset of Figure 13(B) shows that the degradation rate of the non-doped cell dipped below zero at about 39 hours while the degradation rate of the doped cell did not fall below zero until the doped cell had been run for 70 hours. The degradation rates from 40 hours to about 110 hours have been shown in Figure 13(D). This figure indicates that although the degradation rates of the doped and non-doped cells are both less than zero after 40 hours, the magnitude of the degradation rate of the doped cell is greater than -0.2% per hour compared to the degradation rate of the non-doped cell, which is less than -0.2% per hour, and is increasing in magnitude with time even past 100 hours.

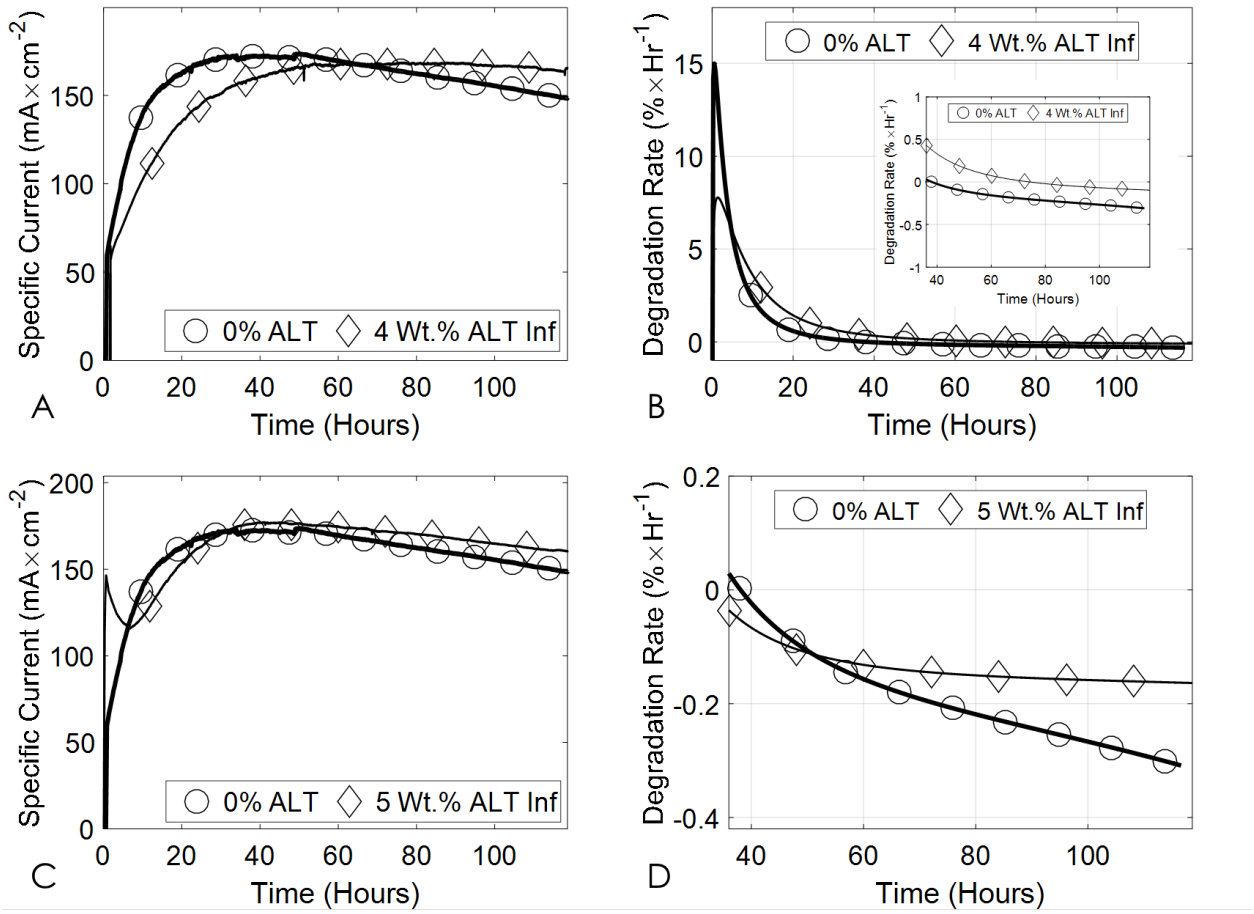

Figure 13: Performance and degradation rate of SOFC anodes fabricated with (diamonds) and without (circles) ALT mechanically mixed into the Ni-YSZ cermet during processing. Cells were run at 800˚C with dry H_2. Data show that ALT-containing anodes consistently out-perform simple Ni-YSZ cermet anodes (without ALT) with lower degradation rates.

2.2.3.A. Testing device durability to electrochemically driven anode oxidation

Redox cycling of cells with pure NiO-YSZ anodes vs. anodes doped with 4 wt% ALT
Experimental Procedure

Cells were heated up to 800 °C (± 5 °C) at 1 °C/min with argon on the anode and air on the cathode. Once at operational temperature, gas flows were adjusted to 100 sccm of argon on the anode and 85 sccm air on the cathode. Initial cell reduction of the anode was performed using 20 sccm of H_2 (in addition to the argon) for one hour. Following this, benchmark linear sweep voltammetry (LSV) and electrochemical impedance spectroscopy (EIS) measurements were acquired at OCV. Once cell performance was known, redox cycling was initiated. Cells were polarized at 50% I_{max} for 20 minutes with 20 sccm H_2 using chronopoteniometric methods monitoring cell voltage. After this, hydrogen was turned off and the anode was allowed to electrochemically oxidize. Final oxidation was determined by a plateau in cell potential and the

re-appearance of NiO in the Raman kinetics. Cells were then re-reduced and benchmark LSV and EIS were collected. These cycles were continued until cell failure which was quantified by a 50% drop in max current. In cases where the cell survived 20 redox cycles under polarization of 50% I_{max} , subsequent cycles were performed at 65% I_{max}.

Schematic of experimental procedure

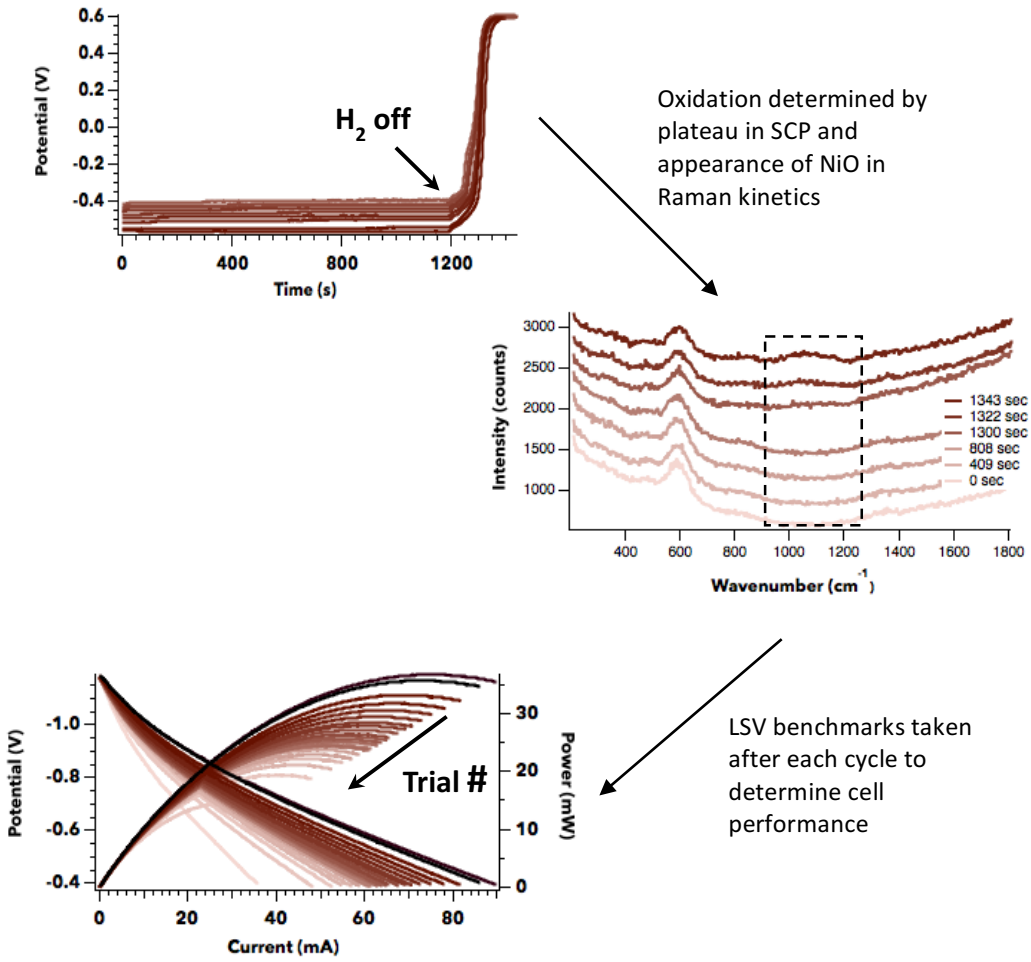

Results

The electrochemical performance of the cells was tested using LSV and EIS following each complete redox cycle. Figure 14 shows that ALT doping helps to increase the resilience and durability of cells to electrochemical oxidation. Cells with standard NiO-YSZ anodes tolerated ~ 15 redox cycles, while cells with ALT doped anodes tolerated over 20 cycles as well as several cycles with increased polarization currents. Upon failure, signs of cell degradation were noticeable in both LSV, by the drop in max current and increase in total resistance (fig 16), and in the EIS by the slight increase in bulk resistance (fig 15). Figure 16 shows total resistance of the cell versus trial number derived from the slope of the current versus potential plots. Cells with doped anodes both maintained lower overall resistances and also show signs of stabilization after cycle 10 and before polarization currents were increased. In addition to the increased resilience of ALT doped anodes, LSV traces suggest a difference in the mechanism of degradation between pure and doped cells. Figure 4 shows a comparison in the LSV traces of a

doped and a pure cell. While the power and current traces of the ALT cell slowly drop in a continuous fashion, the traces for the pure cell seem to cluster intermittently between bigger drops in current and power, perhaps due to the migration and coarsening of Ni particles.

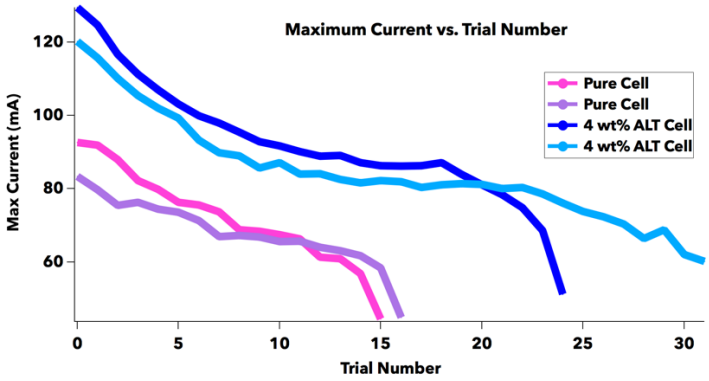

Figure 14. Maximum current measured with LSV versus the trial number

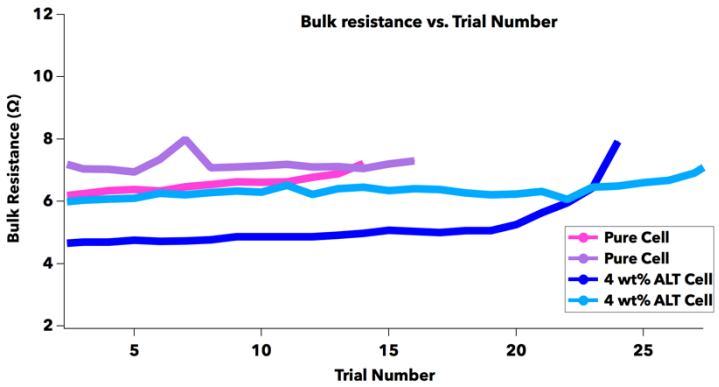

Figure 15. Bulk resistances derived from EIS measurements versus trial number

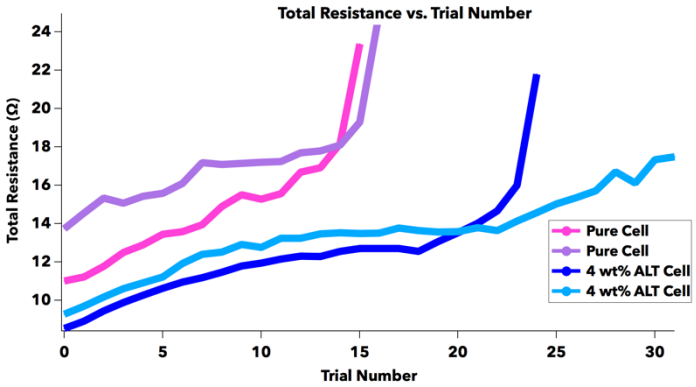

Figure 16. Total resistances derived from current vs. potential slopes versus trial number

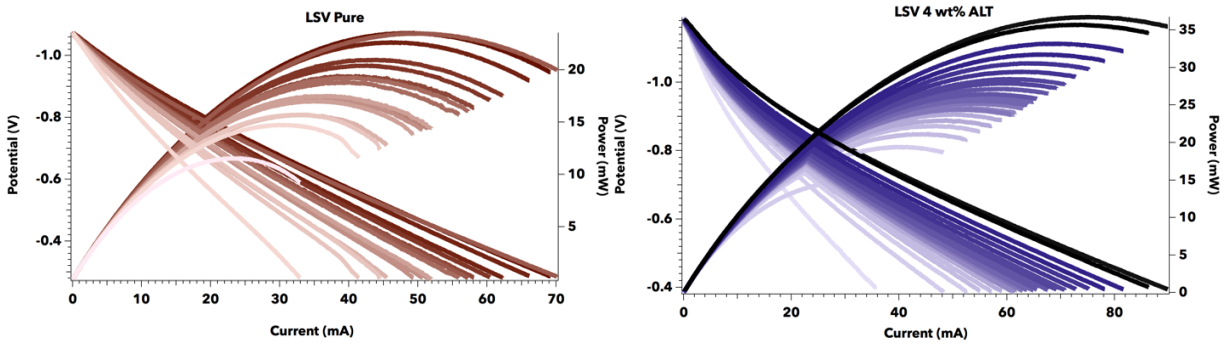

Figure 17. LSV Traces of cell with pure anode (red) and cell with doped anode (blue)

2c. What opportunities for training and professional development has the project provided?

The work described in Section B above has been performed by three graduate students: Clay Hunt, a 4th year Ph.D. student in Montana State's College of Engineering (Mechanical and Industrial) and Ms. Madisen Sickler, a 3rd year Ph.D. student in the newly created Materials Science graduate program and Martha Welander, a 2nd year graduate student in MSU's Department of Chemistry and Biochemistry. These students have been mentored by Professor's Sofie, Amendola and Walker and have learned materials processing skills and developed expertise with material property measurement methods as described above. The team met bi-weekly during the summer months to report progress and setbacks as well as review new, salient literature and discuss both short term and long term activities. Also, 2 undergraduates continued to work on this project. One student, Marley Zahariason, assists Clay Hunt with materials fabrication and SOFC testing. The 2nd student, Joshua Sinrud, is assisting Martha Welander make measurements and prepare cells and has begun exploring the effects of adding TiO_2 and Al_2O_3 separately to Ni-YSZ cermet anodes to isolate the effects of 2° phases on SOFC performance.

2d. How have the results been disseminated to communities of interest?

Opportunities to engage communities of interest came primarily in the form of the SOFC Program Review in June, 2017 outside of Pittsburgh. There, our results were shared and we continued discussions with representatives from Fuel Cell Energy regarding how our studies could best support their continued efforts to develop a more resilient and durable anode material.

2e. What do you plan to do during the next reporting period to accomplish these goals?

This report is the final report for the award period. The Phase 2 proposal describing activities based on the Phase 1 studies was not selected for funding. Nevertheless, in July, we prepared a new Phase 1 proposal that *was* awarded and will build on discoveries made during the previous 24 months. The unsuccessful Phase 2 proposal was judged to not be sufficiently well aligned with the immediate goals and practices of commercial SOFC manufacturers.

Future work carried out under the new award will include a) refining methods used to fabricate anodes from ALT-enhanced Ni-YSZ cermets; b) comparing the performance of ALT-enhanced Ni-YSZ anodes fabricated from mechanically mixed precursors with that of Ni-YSZ anodes that have been modified through ALT infiltration; c) testing the resilience of these novel materials to different oxidative stresses commonly encountered during operation; and d) working closely with an SOFC manufacturer to transfer knowledge learned in our laboratories into full sized cell

fabrication and testing. Meeting these objectives will create a clear roadmap that guides next-generation electrode development for high temperature energy conversion applications.

Specifically, Fabrication of scaled cells for testing by a commercial partner, Fuel Cell Energy, will serves as the final outcome of this proposed activity in which cell composition and structure driven by our laboratory experiments will serve as the framework to prepare commercial scale anode supported SOFCs that can be tested and evaluated with commercial partners. While the preparation of laboratory scale planar anode supported cells limits the challenges associated with warping and curvature, large area geometries present significant challenges to implement new materials and dopants that change the dimensional parameters of the constituents through the entire temperature cycle. Prior results clearly establish both a sintering aid effect and coefficient of thermal expansion (CTE) variation that yields variation with both the concentration of ALT added to the system as well as the size of the nickel oxide precursor. The influence of ALT as a sintering aid plateau's above 5%, in the realm of bulk anode ALT concentrations, will be an important consideration. Below 5%, the influence of ALT on the densification of NiO-YSZ will help optimize anode microstructure.

3. Products

3A. What has the project produced?

This work was presented in an oral presentation at the MS&T Conference in Salt Lake City in October, 2016. One manuscript has been accepted for publication in *Fuel Cells* (M. McCleary, R. Amendola, "Effect of Aluminum Titanate (Al_2TiO_5) Doping on the Mechanical Performance of Solid Oxide Fuel Cell Ni-YSZ Anode", Fuel Cells: from fundamentals to systems, accepted September 5, 2017). Three additional manuscripts are in preparation and will be submitted before the end of the 2017 calendar year: 1) M. D. McIntyre, D. R. Driscoll, J. B. Sinrud, B. D. Gold, M. M. Welander[1], S. S. Sofie, and R. A. Walker "*In situ* Formation of Multifunctional Ceramics: Mixed Ion-Electron Conducting Properties of Zirconium Titanium Oxides" *submitted to J. Materials Chemistry A*; 2) C. Hunt, M. Zachariasen, and S.W. Sofie, "Influence and Optimization of Aluminum Titanate in NiO-YSZ Fuel Cell Anodes"; and 3) M. M. Welander, C. Hunt, M. Zachariasen, S. W. Sofie, and R. A. Walker "Improving Ni-YSZ cermet anode performance in SOFCs through 2˚ phase formation".

3b. Websites

N/A

3c. Technologies or techniques.

Techniques for fabricating SOFC anodes having improved performance and strength are not yet suitably mature to report.

3d. Inventions, patent applications and/or licenses

The Ni-YSZ anodes infiltrated with ALT are still not suitably well described to warrant a patent application.

3e. Other products

N/A

4. Participants and Other Collaborating Organizations

4a. What individuals have worked on the project?

The PI (Walker), two co-PI's (Sofie and Amendola) and two graduate students have all worked on this project.

Participant 1: Dr. Rob Walker
Role: PI
Person months worked: 2
Contribution: Helped plan experiments, analyze data, troubleshoot problems and mentor students
Funding support: Montana State University (during academic year)
Collaborated with individual in foreign country? No

Participant 2: Dr. Stephen Sofie
Role: co-PI
Person months worked: 2
Contribution: Helped plan experiments, devised starting recipes for anode fabrication, analyzed data, troubleshoot problems and mentor students
Funding support: Montana State University (during academic year)
Collaborated with individual in foreign country? No

Participant 3: Dr. Roberta Amendola
Role: co-PI
Person months worked: 2
Contribution: Helped plan experiments, constructed the MOR experimental assembly, analyzed data, troubleshoot problems and mentor students
Funding support: Montana State University (during academic year)
Collaborated with individual in foreign country? No

Participant 4: Mr. Clay Hunt
Role: Graduate student
Person months worked: 9
Contribution: Developed and refined anode fabrication procedures
Funding support: This award
Collaborated with individual in foreign country? No

Participant 5: Ms. Madisen Sickler
Role: Graduate student
Person months worked: 9
Contribution: Performed MOR experiments to assess fracture toughness and began constructing rig for micro-indentation measurements
Funding support: This award
Collaborated with individual in foreign country? No

Participant 6: Ms. Martha Welander
Role: Graduate student
Person months worked: 9

Contribution: Performed *in operando* spectroscopic and electrochemical measurements with pure and ALT doped cells
Funding support: This award
Collaborated with individual in foreign country? No

Participant 7: Ms. Marley Zachariason
Role: Undergraduate student
Person months worked: 3
Contribution: Marley Zachariason, an undergraduate at Montana State University, has been involved with cell fabrication on this project.
Funding support: This award
Collaborated with individual in foreign country? No

Participant 8: Ms. Samantha Lucara
Role: Undergraduate student
Person months worked: 3
Contribution: Samantha hs performed work in the area of sample manufacturing for mechanical testing and fracture analyses
Funding support: This award
Collaborated with individual in foreign country? No

Participant 9: Mr. Joshua Sinrud
Role: undergraduate student
Person months worked: 5
Contribution: Performed *in operando* experiments with Martha Welander.
Funding support: This award
Collaborated with individual in foreign country? No

Participant 10: Mr. Kyle Olson
Role: Undergraduate student
Person months worked: 3
Contribution: Kyle has performed work in the area of ample manufacturing for mechanical testing and fracture analyses
Funding support: This award
Collaborated with individual in foreign country? No

Participant 11: Mr. Quinton Holmlun
Role: Undergraduate student
Person months worked: 3
Contribution: Mr. Holmlund has performed work in the area of frature testing for data analysis.
Funding support: This award
Collaborated with individual in foreign country? No

4b. What other organizations have been involved as partners?

We communicate periodically with colleagues at Fuel Cell Energy, Inc. and used some of that company's raw materials to fabricate ALT-enhanced anodes in the manner described in Sections 2.2.2 and 2.2.3 of this final report.

4c. Have other collaborators or contacts been involved?

N/A

5. Impact

This 18 month project is concluding its 5th quarter, and considerable progress has been made as detailed above. We are in discussions with two companies – Fuel Cell Energy and Atrex – about if/how our labortory discoveries can be tested on a larger scale to discover if ALT doping is a strategy that has commercial viability.

6. Changes/Problems

Thus far, the project has not encountered any problems nor are there any chages to report for project goals.

7. Special Reporting Requirements

This project does not have any special reporting requirements specified in the award terms and conditions.

Budgetary Information

Baseline Reporting Quarter	Q7[a]	Cumulative
Effective date	1/1/17-3/31/17	10/1/15-3/31/17
Baseline cost plan		
Federal share	0	200,000
Non-federal share	0	50,000
Total planned	0	250,000
Actual Incurred cost		
Federal share	1339	200,000
Non-federal share	507	50,000
Total incurred costs	1846	250,000
Variance		
Federal share	(1,339)	0
Non-federal share	(507)	0
Total variance	(1,846)	0

[a]Program was supposed to conclude on 03/31/2017; program continued under no-cost extension through 07/31/2017.